Construction of a Three-Diode-Laser Terahertz Difference-Frequency Synthesizer

Herbert M. Pickett, Pin Chen, John C. Pearson, Shuji Matsuura and Geoffrey A. Blake

Abstract- An all-solid-state, high-resolution and frequency-calibrated THz spectrometer based on optical heterodyne in low-temperature-grown (LTG) GaAs been constructed. [Shuji Matsuura, Pin Chen, Geoffrey A. Blake, John C. Pearson and Herbert M. Pickett, IEEE MTT, in press]. This setup utilizes three distributed-Bragg-reflector (DBR) diode lasers to generate accurate and tunable difference-frequencies in the THz regime. Lasers #1 and #2 are locked to different longitudinal modes of an ultra-low-expansion Fabry-Perot etalon, and laser #3 is offset locked to laser #2, where the offset frequency (ν_{offset}) is set by a microwave sweeper. This three-laser, difference-frequency synthesizer is fully fiber coupled in rigid and compact optical rails. The primary outputs of lasers #1 and #3 pump the LTG GaAs photomixer to generate THz radiation (whose frequency equals to $n \times FSR + \nu_{offset}$, where FSR is the free spectral range of the etalon and n is an integer). The etalon's FSR, and thus the THz frequency, has been calibrated to 50 ppb by acquiring spectra of the 10 rotational lines of CO in the 0.23 to 1.6 THz region.

Index Terms- THz-waves, diode lasers, photomixing, source, calibration

I. Introduction

Advances in laser technology are facilitating a number of new areas of research in physics and chemistry such as the coherent control of matter and a variety of applications involving high-resolution spectroscopy. The generation of coherent light-waves in the terahertz (THz) or far-infrared frequency region has been investigated by many researchers with limited success and presently forms a frontier in optical science [1]. In general, THz frequencies are suitable for the laboratory study of low energy light-matter interactions, such as phonons in solids, rotational transitions in molecules, vibration-rotation-tunneling behavior in weakly bound clusters, electronic fine structure in atoms, thermal imaging of cold sources, and plasma dynamics. In remote sensing applications, sources such as interstellar molecular clouds contain sufficient amounts of cold dust that they are optically opaque. As a result, these sources absorb short wavelength radiation and re-radiate most of it in the THz region, making THz observations of interstellar material in our own galaxy and external galaxies essential for studying the origin and evolution of the universe. Another important remote sensing application is THz studies of the upper reaches of both terrestrial and planetary atmospheres, which also yield critical insights into the nature of atmospheric chemistry and dynamics.

Jet Propulsion Laboratory, California Institute of Technology, Pasadena, CA 91109, USA.

Optical heterodyne mixing (photomixing) in voltage-biased low-temperature-grown (LTG) GaAs photoconductors with planar THz antennas has recently become an attractive frequency down-conversion method because it has demonstrated relatively high conversion efficiency [2,3]. An advantage of the down conversion technique over harmonic generation is that the THz source produced by application of optical/near-IR lasers onto a semiconductor photomixer is widely tunable. Diode-laser-based systems are particularly promising in this type of application since they combine low power consumption and long lifetime in an inexpensive and compact package [4,5]. Such systems have already been applied to laboratory spectroscopy by several authors [6-8]; however, the frequency accuracy of the THz-wave output obtained in previous studies has not been sufficient for high-resolution laboratory spectroscopy or heterodyne remote sensing applications. In this paper we present a method for generating and controlling a near optical difference frequency with the precision necessary far high-resolution applications. Proof of concept is achieved with a LTG photomixing technique. However, the master oscillator power amplifier (MOPA) approach used in the final stage of the system provides sufficient power to take full advantage of the quadratic dependence of the photomixing process on pump laser power [2]. The MOPA can also drive difference frequency generation in any good nonlinear optical materials should they become available. It should be further noted that this method of frequency control can be used at any optical or infrared wavelength where suitable lasers and optics exist. Laser System Design and Performance

A. General Concept

The light source of the difference frequency system consists of three diode lasers, as is depicted in Fig. 1. Each laser diode is outfitted with collimating lens, a length tunable external-cavity assembly, and the necessary optics to circularize and fiber couple the optical radiation. Alignment is maintained by a compact aluminum rail structure. All the optical signal- processing components are implemented in polarization maintaining (PM) single-mode fiber. The optical components used and their layout is shown in Fig. 1. Commercial components were used whenever available, but some home made components were necessary. The fiber optic approach offers flexibility, compactness, insensitivity to vibration, ease of optical alignment, and eye protection. The optical fiber also serves as a spatial filter, allowing two different laser frequencies to be combined with nearly perfect spatial mode overlap. The latter is critical in the Fabry-Perot etalon alignment, in achieving equal amplification in the

final MOPA, and in efficient photomixer operation. The major drawbacks of the fiber-based optical system as opposed to a free space system are the increased cost and the optical insertion losses of the PM fiber. Due to the coupling losses, the output power of the present laser system was insufficient to optimally pump the photomixer used to generate THz-waves. As a result, a MOPA amplifier was employed as the final optical element before the photomixer once it had been determined that the spectral properties of the seed lasers were preserved in the amplification process [14].

Frequency control is achieved by locking two of the lasers (#1 and #2) to different longitudinal modes of an ultra-low-expansion (ULE) Fabry-Perot (FP) etalon. The difference frequency between the two cavity-locked lasers is discretely tunable in steps of the cavity free spectral range (FSR). The third laser (#3) is heterodyne phase-locked to one of the cavity-locked lasers (#2) with a tunable 3-6 GHz microwave synthesizer. The difference frequency between the #1 and #3 lasers is determined by the sum of integral multiples of the FSR (3 GHz in the present system) of the reference cavity and the microwave offset frequency. The accuracy of the difference frequency is determined by the accuracy of the FSR measurement along with any DC offset in the electrical portions of the lock loops. The microwave offset frequency is locked to a high accuracy (1 in 10^{-12}) reference source and measured by a counter locked to the same reference in order to correct in real time any electrical offset in that lock loop. The ULE material has a thermal expansion coefficient at room temperature of $\alpha = -2 \times 10^{-10}\ C^{-1}$, which is comparable to the stability of a good quartz reference oscillator in conventional microwave sources. As will be described later, the measurement of molecular transitions allows any DC offsets in the two cavity lock loops to be determined and the system to be calibrated to very high precision. The optical and electrical details of all the major sub-systems

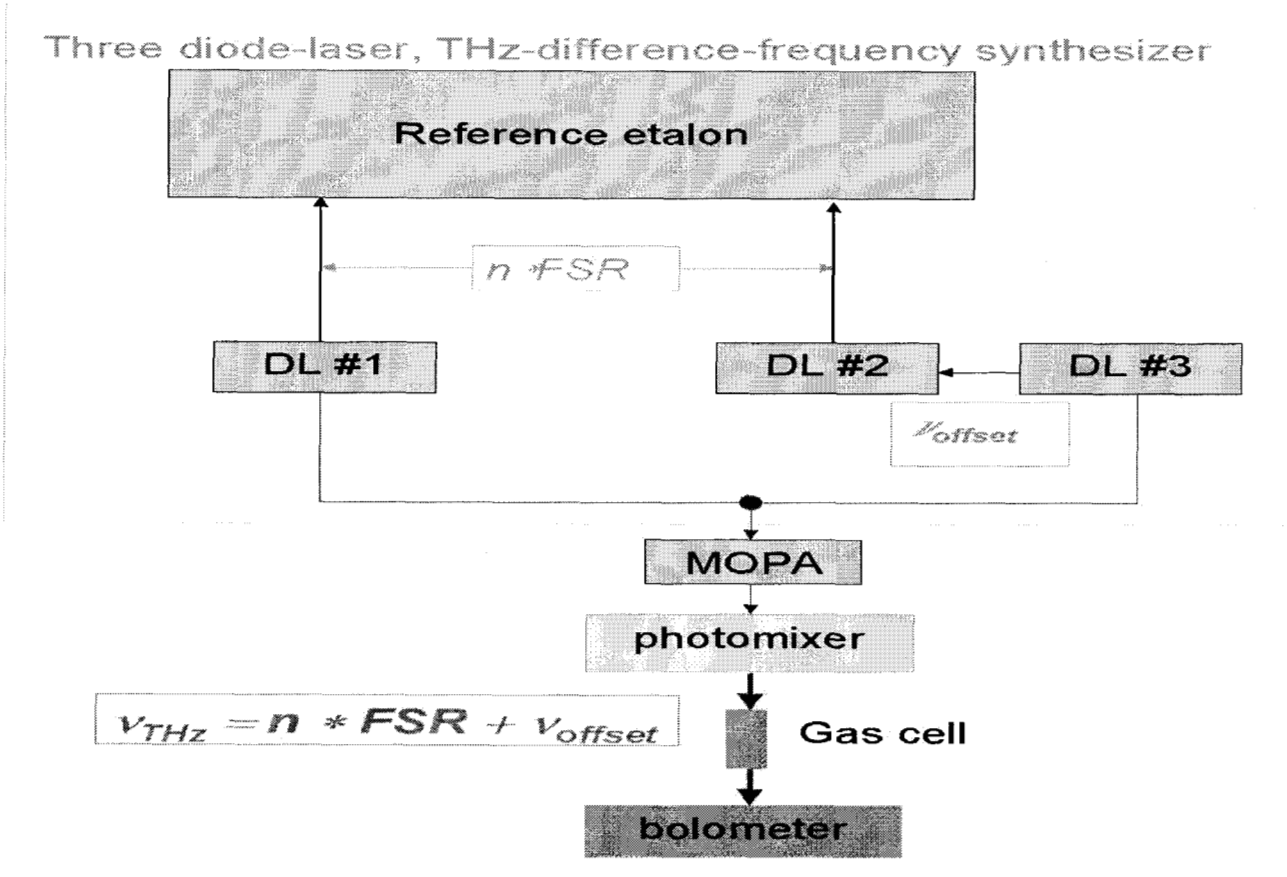

Figure 1: Overall Block Diagram

of this THz difference frequency generator are described in the next few sections in detail.

B. Laser Assembly and Control

The full schematic of the external-cavity diode laser assembly is presented in Fig.2. The assembly consists of an SDL3722 852 nm, 150 mW, distributed Bragg reflector (DBR) diode laser, an f = 4.5 mm collimating lens, an external cavity comprised of a 4% partial reflector mounted on a piezoelectric transducer (PZT), an anamorphic prism pair, a 60-dB optical isolator, an f = 8 mm optic, and a adjustment flexure for fiber coupling. A rooftop mirror glued onto a 20% beam splitter cube forms the actual external cavity. The edge of the rooftop mirror is oriented along the short axis of the elliptical beam from the DBR laser, which is more sensitive to the tilt angle than is the long axis. As such, the round-trip mirror configuration offers relatively alignment-free optical feedback. The reflector and the DBR laser chip constitute an external-cavity with a length of approximately 50-mm. The 3:1 aspect ratio beam transmitted through the partial reflector is circularized by the anamorphic prism pair to achieve better spatial overlap with the PM fiber and thereby improve the coupling efficiency. These components are assembled in a 250-mm long aluminum rail to maintain alignment. The typical optical power coupled into the PM fiber was approximately 30% of the original power emitted from the DBR laser. The transmission of the free-space optics in the laser assembly was measured at ~70% and the fiber-coupling efficiency was typically ~50%. The theoretical maximum fiber-coupling efficiency calculated from the measured beam size and the fiber core size is 60% of the DBR power. The best coupling ever achieved by this optical system was 55%. Other power losses include the use of a passive 3-dB directional coupler to combine the output laser beams and ~1-dB losses at each fiber connector. As a result the typical power available at the MOPA is ~30 mW, with the best ever achieved being ~53 mW. The difference in the typical and maximum powers is due to slight thermal deformations in the rail assembly and the slow buildup of dust and dirt in the fiber connectors over time.

The DBR diode laser coupled to the external-cavity oscillates at the cavity mode that is the closest to the gain maximum of the DBR laser. The FSR of the external cavity was ~3 GHz, corresponding to the separation between the partial reflector and the DBR chip. The laser frequency is continuously tunable since the external cavity's FSR can be tuned by the PZT at the rate of 160 MHz/V. The continuous PZT tuning range is limited by mode hops to different transverse modes favored by the gain profile of the DBR laser. In order to avoid such mode hops, the laser's temperature can be adjusted to maximize its gain at the external-cavity mode frequency, completely suppressing the mode hops and facilitating continuous tuning over the PZT tuning limit of 5 GHz . Coarse frequency tuning spanning > 700 GHz is available by changing the laser temperature over the range of 5-30 C (or 27 GHz/K). Although the injection current also affects the laser frequency (> 600 MHz/mA), the current was normally set to be constant unless fine or fast frequency tuning is necessary.

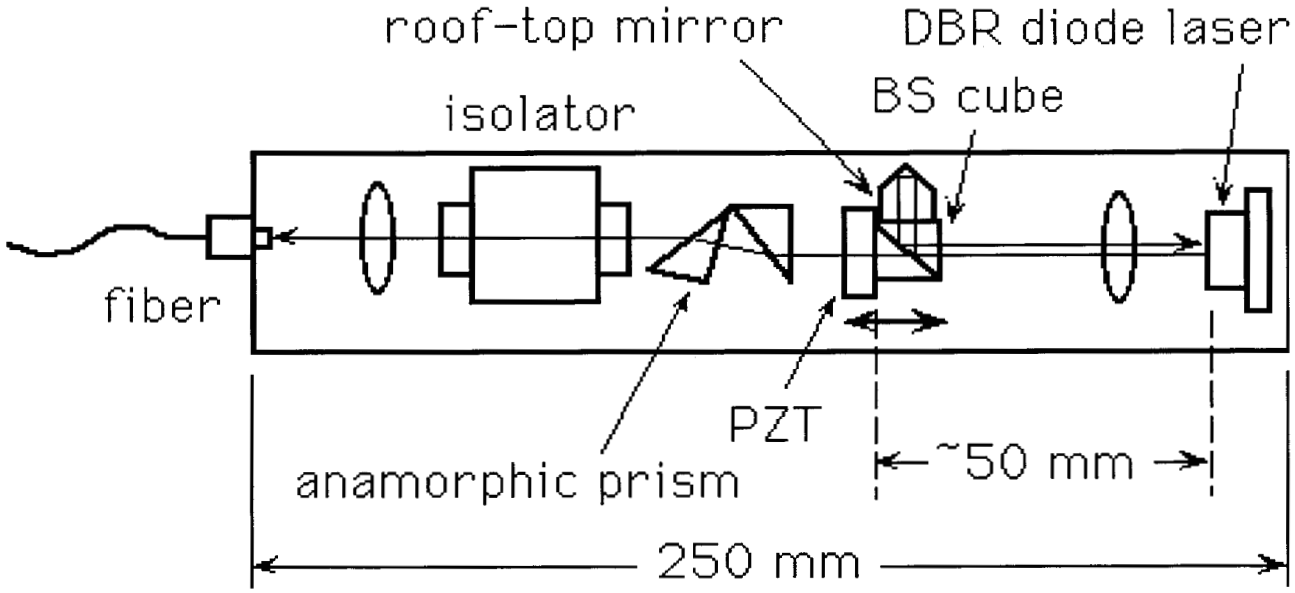

Figure 2: Diode Laser Assembly

Stable diode laser operation requires that both the injection current and the temperature be precisely controlled. A low cost, high performance control circuit has been designed in order to satisfy the control criteria. The current controller was adapted from Libbrecht and Hall's work [9] to suit the anode-ground configuration of the DBR lasers. The laser temperature is stabilized by a bridge circuit incorporating both differential drive and detection using the DBR laser's built in thermistor and

thermoelectric cooler. The current supply, the temperature controller, and the PZT controller, including the frequency stabilization circuit, are fabricated on a 4 x 6 inch circuit board and interfaced with a computer through a serial interface for monitor and control purposes. This single board design has the advantages of compactness, high performance, and low cost.

In spite of the much lower level of optical feedback than that of conventional external-cavity diode lasers, a significant narrowing of the laser linewidth was realized. The linewidth measured by the delay-line self-heterodyne technique was narrower than 500 kHz FWHM, which is near the spectral resolution limit imposed by the optical delay length of 200 meters. This linewidth is a significant improvement over the free running DBR Linewidth of several to several tens of MHz. According to a previous study on the frequency stability of diode lasers at various feedback levels [10], our case falls into the weak feedback regime where stable single-mode narrow-line oscillation should be observed.

C. *Frequency Stabilization*

The P1 and P2 lasers were cross-polarized in order to allow them to be locked to different longitudinal modes of the ULE etalon by the Pound-Drever-Hall method [11,12]. FM sidebands were generated on the two cavity-locked lasers with electro-optic phase modulators (EOM) operating at 80 MHz and 120 MHz. The modulation index was chosen to maximize the phase shift seen in the reflection from the cavity. To verify coupling to the fundamental longitudinal cavity mode, the transmitted beam profile was monitored by a CCD-camera. Since density and humidity changes in air can cause FRS fluctuations through refractive index changes, the cavity was installed in a sealed box, which was evacuated and then back filled with dry nitrogen so that the density inside the box was constant. The phase of the beam reflected from the cavity was compared to the modulation frequency in a frequency multiplier (Analog Devices 834Q). When the laser frequency is within the modulation frequency of the cavity resonance, the output of the frequency multiplier provides a DC frequency dispersion that crosses zero at the cavity resonance. The central linear portion of the dispersion curve centered at the cavity is used to generate an error signal voltage, which is fed back to the PZT of the external laser cavity with a simple servo electronic circuit consisting of an integrator and an amplifier. The Linear part of frequency discriminator is ~4 MHz, in accordance with the FSR of the cavity of 3 GHz and its finesse of 750. The pull-in range of this locking method is limited by the distance to the upper and lower sidebands, or 2x modulation frequency (160 and 240 MHz). In the present laser system, the loop bandwidth of the PZT control circuit was limited to 3 kHz to avoid acoustic resonances in the support structure of the partial reflector and the PZT. It was observed that only 200 Hz of bandwidth was required for stabilization, but the additional bandwidth was retained to facilitate sweeping of the offset laser.

The offset-locked laser is locked to a beat note signal between the # 2 and #3 lasers detected by a 6 GHz bandwidth photodetector and compared to tunable frequency generated by a microwave synthesizer. In order to implement a phase-lock with the same electronics as the cavity-lock, the signal was split with one arm sent through a delay line, and the resulting phase shift between the two signals was used to generate the error signal for the PZT of the #3 laser. The delay line has an effective reference frequency of 71.9 MHz; however, concerns about the accuracy and stability of this effective lock frequency led to the use of a counter. The offset frequency is measured precisely by a microwave counter locked to a high precision reference, making any drifts or offsets in the phase lock scheme irrelevant to the system calibration. The offset frequency can be continuously tuned over 5 GHz by stepping the synthesizer frequency and tracking the PZT voltage. The maximum sweep rate of <100 MHz/sec is limited by the feedback loop bandwidth.

The overall system performance was assessed by observing a beat note between the #1 and #3 lasers with a 25 GHz bandwidth photodetector and a spectrum analyzer. Fig. 3 shows a 12 GHz beat spectrum for a 1-second integration time and a spectral resolution of 100 kHz. The FWHM spectral power bandwidth is approximately 800 kHz. This result confirms the self-heterodyne linewidth measurement of ~500 kHz. The short-term linewidth of each laser is determined entirely by the optical feedback from the external cavity because the 3 kHz bandwidth of the lock loop circuit is much less than the laser linewidth. DBR linewidths of ~50 kHz have been achieved by weak optical feedback from FP-cavities [6]. The additional narrowing is due to 180-degree phase shift over a narrow (60 MHz) cavity width compared with the same phase shift over 1.5 GHz in the scheme presented here. Fast electronic feedback to the laser current can also be used to narrow the laser linewidths [13], but the DBR lasers used here have some unfortunate characteristics that made this impractical.

D. *Dual-Frequency MOPA operation*

Since the typical output power of the fiber-coupled laser system is ~30 mW, it was not sufficient to efficiently generate THz radiation by photomixing As a result we amplified the dual-frequency signal with a MOPA. Dual-frequency MOPA operation has the advantages of high power output and guarantees excellent spatial overlap of the two frequency beams, which is essential for efficient optical-heterodyne conversion.

The MOPA amplifier system was a single traveling-wave 850-nm semiconductor tapered optical amplifier, which was the central component of a commercial external-cavity single-mode laser (SDL8630). The dual-frequency fiber output from the three laser system was collimated by an f = 8 mm collimating lens, passed through a 60-dB optical isolator, and sent to a half-wave plate for fine adjustment of the polarization. The circular beam was transformed into an elliptical shape by an anamorphic prism pair in order to match its spatial mode to the amplifier 1 x 3 μm input facet. After appropriate attenuation, the beam is injected into the optical amplifier chip through another f = 8 mm focusing lens. The output beam from the amplifier is spatially filtered and collimated to a 3 mm diameter Gaussian beam by a

telescope. A detailed description of the dual-frequency MOPA system has been given elsewhere [14].

II. THz-wave Generation

As described in the Introduction, the dual-frequency laser system can generate THz-waves by difference frequency mixing in LTG-GaAs ultra-fast photoconductors or other nonlinear optical media. Here, we demonstrate the performance of the laser system with high-resolution rotational spectroscopy of the simple molecules acetonitrile (CH_3CN) and carbon monoxide (CO). Due to the lack of spectral analysis techniques in the THz region, spectroscopic measurements provide one of the best diagnoses of frequency and spectral purity, which is essential if this source is going to be useful as a local oscillator.

A. *Spectroscopy*

The LTG-GaAs photomixer used in the present experiment was grown on a semi- insulating GaAs substrate, and a planar log-spiral antenna with 0.2-μm interdigitated electrodes and 1.5-μm gaps in a 8 x 8 -μm active area was etched on the wafer [16]. The photomixer was mounted on the flat surface of a 10 mm diameter hyper-hemispherical lens made of high-resistivity silicon. Most of the radiation generated by the antenna and electrodes passes into the photomixer substrate and through the Si lens. A DC bias voltage of 20 V was applied to the electrodes by a constant current supply set at 0.5 mA for a laser input power of 30 mW. Under these conditions, the photomixer provided a maximum output power of ~0.1 μW at 1 THz, while the 3 dB bandwidth of the generated THz waves was approximately 700 GHz, as is shown in Fig. 7. The spectral bandwidth and the frequency roll-off behavior is roughly consistent with the carrier lifetime of the LTG-GaAs of $\tau \sim$ 200-300 fs and the photomixer RC time constant, where R = 72 Ω is the radiation impedance and C = 0.5 fF is the electrode capacitance [16].

B. *Frequency Calibration*

For further spectroscopic measurements such as the search for unknown molecular lines and for use in astronomical observations, absolute frequency calibration of the difference frequency is necessary. Since the accuracy of the difference frequency is defined by the reference FP-cavity, the calibration must include a precise measurement of the FSR of the cavity. Once the exact value of the FSR is obtained, the difference frequency can be determined, in principle, to within an accuracy of $\sim 10^{-10}$, if temperature fluctuations of the cavity are kept below ~1 C, because of the extremely low thermal expansion coefficient of the ULE material. The FSR of the FP-cavity was initially measured by detecting the beat signal between the two cavity-locked lasers (#1 and #2) with a microwave counter. In this measurement, the FSR was determined to be 2996.71 ± 0·05 MHz. The laser linewidth and an electrical offset of the phase-lock loop circuit limited the accuracy of this measurement. Well known molecular lines in the THz region, such as the rotational transitions of carbon monoxide (CO), are suitable for more accurate calibration, since the frequencies of these THz molecular transitions correspond to ~300 times the FSR and can be easily measured to within an accuracy of 10^{-7}. A number of measurements and the careful use of statistics should allow for a rapid calibration of 10^{-8}. Other FSR measurements have been proposed and demonstrated to better than 10^{-10} by [18], but these require the use of expensive fast EOMs matched to the cavity FSR.

Pure rotational transitions of CO were measured using the configuration shown in Fig. 1. A composite silicon bolometer was used in these. According to the conventional model for the diatomic $^{12}C^{16}O$ molecule, the rotational transition lines should appear at frequencies of $\nu = (W_{J+1} - W_J) / h$, and $W_J / h = B\,J(J+1) - D\,J^2(J+1)^2 + H\,J^3(J+1)^3$, where B = 57,635.9660 MHz, D = 0.1835053 MHz, $H = 1.731 \times 10^{-7}$ MHz, h is Planck constant, and J is an integer [19]. Absorption measurements for CO lines with J_{lower} = 1-10 over the range of 230 GHz to 1267 GHz were carried out by measuring the microwave offset frequency, ν_{offset}, and counting the number of cavity orders between the two cavity-locked lasers. The line position was determined by fitting a parabola to the center of the 2nd derivative line profile. The measured and calculated rotational frequencies and their differences are summarized in Table 1.

TABLE 1

Measured and Calculated CO Rotational Frequencies

Calculated [MHz]	Measured [MHz]	Difference [MHz]
230538.00	230537.88	-0.12
345795.98	365795.95	-0.03
461040.75	461040.90	0.15
576267.91	576268.03	0.12
691473.05	691473.06	0.01
806651.77	806651.60	-0.17
921799.67	921799.85	0.18
1036912.35	1036912.80	0.45
1151985.40	1151985.34	-0.06
1267014.44	1267014.10	-0.34

The final measured frequencies were obtained using the calibrated FSR value of the cavity as follows: The cavity FSR for each CO line is simply calculated by dividing $\nu - \nu_{offset}$ by the cavity order difference, because the DC offset of the difference frequency caused by the DC offset voltage of the lock loop circuit was statistically insignificant. From this data set, the average of the FSR value for all CO line measurements was determined to be 2,996,757.48 ± 0·10 kHz. It should be noted that the FSR could be a function of cavity order due to dispersion of the refractive index of the cavity coatings. However, no variations are convincingly observed and the expected effect is smaller than the current precision [18].

C. *Conclusions*

The photomixer used in the experiments reported, here provides a maximum output power of approximately 0.1 μW at 1 THz for a pump laser power of 30 mW. A

straightforward extrapolation of the quadratic dependence of the THz-wave power on the laser power leads to the prediction that some 10 μW of power should be obtainable using the present laser system, whose maximum 850 nm power is 500 mW. However, the maximum pump laser power is currently limited to approximately 50 mW by thermal failure of the photomixer [14], and the output power measured in previous work has therefore been limited to levels of <1 μW [3,8,16]. To solve this thermal problem, photomixers with distributed electrode structures and higher thermal conductivity substrates are being developed [16,20]. Such photomixers can be driven at the full output of the high-power laser system reported here, and will ultimately produce power levels of nearly 10 μW at 1 THz. Larger frequency offsets are easily obtained with additional DBR lasers or by using grating-tuned external cavity diode lasers [15]. The current power levels are already sufficient for spectroscopic applications in the 3-6 THz region if more sensitive detectors than those available here are used (e.g., Ga:Ge photoconductors or bolometers with superconducting coupling antennae).

The three-laser difference frequency generation and control method presented here is quite general and could be extended to a large number of different lasers. The absolute calibration method is also quite general and can be widely employed, as long a method of generating a THz-wave output is available. This frequency control technique is especially important in the >1-2 THz region, where comparison to a harmonically up-converted frequency reference may be difficult or impossible. The use of a MOPA as a dual-frequency amplifier should facilitate the use of this control method with the next generation of photomixers based on nonlinear optical media such as $LiNbO_3$, GaP, GaAs, and quantum-well materials. At optical source frequencies down-conversion methods using nonlinear optical materials might be more efficient than electro-optical down-conversion with photoconductors because the efficiency of the optical down-conversion, in general, has a ν^4 dependence in the long-wavelength limit [21]. The present laser system design provides the necessary control to take advantage of any improvements in conversion efficiency using such methods. Further development of nonlinear optical materials and novel devices with large χ^2 at diode laser frequencies are also expected in the near future, making precision difference frequency generation essential for their use as THz sources.

Finally, the type of THz source demonstrated here should be useful not only for THz spectroscopy but also as local oscillators (LOs) for future airborne and space-borne THz heterodyne receivers to be used in atmospheric science and astronomy. The advantage of space-bone telescopes in the THz range is their continuous, wide frequency coverage, which is prevented by strong atmospheric water line absorption at low altitudes. The wide tunability of a photomixer-based LO system will make it possible to construct highly tunable heterodyne receivers with a single local oscillator and a single mixer. Properties of the present laser system such as its small size, low power consumption, and fiber-connectorized optics also make it highly suitable for space-borne instruments. The development of such remote sensing THz spectrometers is currently in progress.

Acknowledgements
The authors thank S. Verghese and K. A. McIntosh of MIT Lincoln Laboratory for preparing the LTG-GaAs photomixers. We also thank T. J. Crawford of Jet Propulsion Laboratory for his technical support. Portions of this work performed at the Jet Propulsion Laboratory California Institute of Technology were done under contract with the National Aeronautics and Space Administration (NASA). G. A. Blake acknowledges additional support from NASA and from the National Science Foundation.

References

1. R. Datla, E. Grossman, and M.K. Hobish, eds., *Metrology Issues in Terahertz Physics and Technology*, NIST vol., 5701, 103 pp., 1995.
2. E. R. Brown, F. W. Smith, and K. A. McIntosh, "Coherent Millimeter-Wave Generation by Heterodyne Conversion in Low-Temperature-Grown GaAs Photoconductors," *J. Appl. Phys*, vol. 73, pp. 1480-1484, 1993.
3. E. R. Brown, K. A. McIntosh, K.B. Nichols, and C.L. Dennis, "Photomixing up to 3.8 THz in Low-Temperature-Grown GaAs," Appl. Phys. Lett., vol. 66: pp. 285-287, 1995.
4. K. A. McIntosh, E. R. Brown, K. B. Nichols, O. B. McMahon, W. F. DiNatale, and T. M. Lyszczarz, "Terahertz Photomixing With Diode-Lasers in Low-Temperature-Grown GaAs," *Appl. Phys. Lett.*, vol. 67, pp. 3844-3846, 1995.
5. S. Matsuura, M. Tani, and K. Sakai, "Generation of Coherent Terahertz Radiation by Photomixing in Dipole Photoconductive Antennas," *Appl. Phys. Lett.*, vol. 70, pp 539-561, 1997.
6. A. S. Pine, R. D. Suenram, E. R. Brown, and K. A. McIntosh, "A Terahertz Photomixing Spectrometer - Application to SO_2 Self-Broadening, *J. Mol. Spec.*, vol. 175, pp. 37-47, 1996.
7. P. Chen, G. A. Blake, M. C. Gaidis, E. R. Brown, K. A. McIntosh, S. Y. Chou, M. I. Nathan, and F. Williamson, "Spectroscopic Applications and Frequency Locking of THz Photomixing with Distributed-Bragg-Reflector Diode Lasers in Low-Temperature- Grown GaAs," *Appl. Phys. Lett.*, vol. 71, pp. 1601-1603, 1997.
8. S. Matsuura, M. Tani, H. Abe, K. Sakai, H. Ozeki, and S. Saito, "High Resolution THz Spectroscopy by a Compact Radiation Source Based on Photomixing with Diode Lasers in a Photoconductive Antenna," *J. Mol. Spec.*, vol. 187, pp. 97-101, 1998.
9. K.G. Libbrecht and J. L. Hall, "A Low-Noise High-Speed Diode Laser Current Controller," *Rev. Sci. Instr.*, vol. 64, pp. 2133-2135, 1993.
10. R.W. Tkach and A.R. Chraplyvy, "Regimes of Feedback Effects in 1.5 μm Distributed Feedback Lasers," *IEEE J. Lightwave Technol.*, vol. LT-4, 1635-1661, 1986.
11. R. V. Pound, *Rev. Sci. Instrum.*, vol. 17, pp. 490-505, 1946.
12. R. W. P. Drever, J. L. Hall, F. V. Kowalski, J. Hough, G. M. Ford, A.J. Munley, and H. Ward, "Laser Phase

and Frequency Stabilization using an Optical Resonator," *Appl. Phys. B,* vol. 31, pp. 97-105, 1983.
13. L. Hollberg, V. L. Velichansky, C. S. Weimer, and R. W. Fox, "High-Accuracy Spectroscopy with Semiconductor Lasers: Application to Laser-frequency Stabilization," in *Frequency Control of Semiconductor Lasers*, M. Ohtsu, ed.: pp. 73-93, New York: Wiley, 1996.
14. S. Matsuura, P. Chen, G. A. Blake, J. C. Pearson, and H. M. Pickett, "Simultaneous Amplification of Terahertz Difference Frequencies by an Injection-Seeded Semiconductor Laser Amplifier at 850 nm," *Int. J. of Infrared and Millimeter Waves*, vol. 19, pp. 849-858, 1998.
15. D. Wandt, M. Laschek, F. v. Alvensleben, A. Tunnermann: and H. Welling, "Continuously Tunable 0.5 W Single-Frequency Diode Laser Source," *Opt. Commun.*, vol. 145, pp. 261-264, 1998.
16. S. Verghese, K. A. McIntosh, and E. R. Brown. "Highly Tunable Fiber-Coupled Photomixers with Coherent Terahertz Output Power," *IEEE Trans. Microwave Theory and Tech.*, vol. 45, pp. 1301-1309. 199T.
17. H. M. Pickett, "Determination of Collisional Linewidths and Shifts by a Convolution Method," *Appl. Optics*, vol. 19, 2745-2749: 1980.
18. R. G. DeVoe, C. Fabre, K. Jungmann, J. Hoffnagle, and R. G. Bremer, "Precision optical-frequencv-difference measurements," *Phys. Rev. A*, vol. 37, 1802-1805, 1988.
19. I. Nolt, J. V. Radostitz, G. Dilonardo, K. M. Evenson, D. A. Jennings, K. R. Leopold, L. R. Zink. and A. Hinz, "Accurate Rotational Constants of CO: HCl, and HF - Spectral Standards for the 0.3 to 6 THz (10 cm^{-1} to 200 cm^{-1}) Region,:' *J. Mol. Spec.*, vol. 125, pp. 274-287, 1987.
20. L.Y. Lin, M. C. Wu, T. Itoh, T. A. Vang, R. E. Muller, D. L. Sivco, and A. Y. Cho. "Velocity-Matched Distributed Photodetectors with High Saturation Power and Large Bandwidth." *IEEE Photon. Technol. Lett.*, vol. 8, pp. 1376-1378, 1996.
21. Y. R. Shen, *Principles of Nonlinear Optics*. New York: John Wiley and Sons, 1984.